C. R. Geoscience 351 (2019) 197–208

Contents lists available at ScienceDirect

Comptes Rendus Geoscience

www.sciencedirect.com

Internal Geophysics (Physics of Earth's Interior)

On the implications of the coupled evolution of the deep planetary interior and the presence of surface ocean water in hydrous mantle convection

Takashi Nakagawa [a,*], Hikaru Iwamori [b,c,d]

[a] Department of Earth Sciences, University of Hong, Pokfulam Road, Hong Kong
[b] Department of Solid Earth Geochemistry, Japan Agency for Marine-Earth Science and Technology, 237-0061 Yokosuka, Japan
[c] Department of Earth and Planetary Sciences, Tokyo Institute of Technology, Meguro, 152-8581 Tokyo, Japan
[d] Earthquake Research Institute, University of Tokyo, Bunkyo, 113-0032 Tokyo, Japan

ARTICLE INFO

Article history:
Received 20 March 2018
Accepted after revision 8 February 2019
Available online 2 April 2019

Handled by Yanbin Wang

Keywords:
Core–mantle evolution
Hydrous mantle convection
Ocean

ABSTRACT

We investigate the influence of the deep mantle water cycle incorporating dehydration reactions with subduction fluxes and degassing events on the thermal evolution of the Earth as a consequence of core–mantle thermal coupling. Since, in our numerical modeling, the mantle can have ocean masses ~12 times larger than the present-day surface ocean, it seems that more than 13 ocean masses of water are at the maximum required within the planetary system overall to partition one ocean mass at the surface of the present-day Earth. This is caused by effects of water-dependent viscosity, which works at cooling down the mantle temperature significantly so that the water can be absorbed into the mantle transition zone and the uppermost lower mantle. This is a result similar to that without the effects of the thermal evolution of the Earth's core (Nakagawa et al., 2018). For the core's evolution, it seems to be expected for a partially molten state in the deep mantle over 2 billion years. Hence, the metal–silicate partitioning of hydrogen might have occurred at least 2 billion years ago. This suggests that the hydrogen generated from the phase transformation of hydrous-silicate-hosted water may have contributed to the partitioning of hydrogen into the metallic core, but it is still quite uncertain because the partitioning mechanism of hydrogen in metal–silicate partitioning is still controversial. In spite of many uncertainties for water circulation in the deep mantle, through this modeling investigation, it is possible to integrate the co-evolution of the deep planetary interior within that of the surface environment.

1. Introduction

The deep mantle water cycle has been discussed with regard to various implications on the properties of silicate materials, which can host water at high pressures and temperatures (e.g., Karato, 2011), and the amount of water that the mantle from the early to the present Earth can contain has been examined (Rüpke et al., 2004; Sandu et al., 2011). A series of our studies on hydrous mantle convection models have focused on the mantle water cycle, including the dehydration reactions associated with water solubility in mantle minerals (Nakagawa and Spiegelman, 2017; Nakagawa et al. (2015)) and the effects of the occurrence of surface plate motions and water absorption in the mantle transition zone (Nakagawa and Iwamori, 2017). These studies also noted that heat transfer

* Corresponding author.
E-mail address: ntakashi@hku.hk (T. Nakagawa).

https://doi.org/10.1016/j.crte.2019.02.001
1631-0713/

during hydrous mantle convection might be enhanced by approximately 30% compared with that during dry mantle convection due to viscosity reduction and enhancement of surface plate motion associated with water dependence of viscosity. In a coupled core–mantle evolution modeling, this has been mainly done in dry mantle convection simulations (e.g., Nakagawa and Tackley, 2010), but not in hydrous mantle convection simulations. The question is how the material properties of the hydrous mantle (e.g., water-dependent viscosity) affect the coupled core–mantle evolution.

Regarding hydrous mantle convection modeling, several parameterized models of mantle heat transfer with water migration have been investigated assuming coupled ocean–plate–mantle evolution (Korenaga, 2011; Rüpke et al., 2004; Sandu et al., 2011), which suggested that water in the planetary system (both in the exosphere and in the deep interior) may contain several times the present-day amount of surface seawater (1.4×1021 kg; e.g., Genda, 2016); however, those studies did not discuss the impacts on core evolution, the effects of dehydration reactions on mantle water migration, and the dynamical effects of mantle convection. Without core evolution effects, it seems that a planetary system assuming water solubility effects during hydrous mantle convection may contain at least 6 to 12 ocean masses of water at maximum (Nakagawa et al., 2018), which seems to be consistent with petrological estimates of 8 to 12 ocean masses (Iwamori, 2007). Note that this estimate is the maximum value, but, due to geological and geochemical constraints for water in the Earth's mantle, it seems that the mantle may contain less water than indicated in the above statements because only small sea level change would be expected (Korenaga et al., 2017; Parai and Mukhopadhyay, 2012) and because of the evolution of the D/H ratio (Kurokawa et al., 2018), which would be 1 to 2 ocean masses in the mantle. This question remains controversial.

The effects of the thermal evolution of the planetary core in a hydrous mantle convection system must still be discussed to give a better understanding of the evolution of the deep planetary interior. It would be worth to investigate how hydrous mantle convection affects the thermal and chemical evolution of the core–mantle boundary (CMB) to reveal the physical and chemical processes involved in the core–mantle–plate–ocean system; this means that we may add constraint, that is, the present-day amount of surface seawater, into the previous core–mantle evolution model. Here, we introduce a new successful scenario of the thermal and chemical evolution of the deep planetary interior and ocean in hydrous mantle convection. Moreover, as a consequence of our modeling results, the hydrogen cycle across the deep Earth's interior could be implied with the core–mantle chemical interactions by the metal–silicate partitioning of hydrogen (Okuchi, 1997), because recent accomplishments in high *P-T* experiments suggest that iron and water-bearing minerals might be stable at lower mantle conditions (Nishi et al., 2017) and that hydrogen might also be generated by the chemical reactions of such minerals (Hu et al., 2016) and could be partitioned into bridgmanite-post-perovskite (Townend et al., 2016).

1.1. Model description

In this study, we use a modified version of the coupled core–mantle evolution model used in Nakagawa and Tackley (2010). The modified core–mantle evolution model includes the effects of water migration and the partitioning of water into the molten mantle, as described in Nakagawa et al. (2015) and Nakagawa and Spiegelman (2017). A more detailed formulation of the model is given in the Appendices A1 to A3. Here, we briefly introduce these points.

For the modeled mantle, we assumed a compressible and truncated anelastic approximation with temperature-, pressure-, and water-dependent viscosity given as follows:

$$\eta_{\mathrm{d}} = A_{\mathrm{d}} \sum_{i,j=1}^{n_{\mathrm{phase}=3,4}} \Delta\eta_{i,j}^{r_{ij}f_j} \exp\left[\frac{E_{\mathrm{d}} + pV_{\mathrm{d}}}{RT}\right] \tag{1}$$

$$\eta_{\mathrm{w}} = A_{\mathrm{w}} \left(\frac{c_{\mathrm{w}}}{c_{\mathrm{w,ref}}}\right)^{-1^{\mathrm{n}}_{\mathrm{phase}=3,4}} \sum_{i,j=1} \Delta\eta_{ij}^{\Gamma_{ij}f_j} \exp\left[\frac{E_{\mathrm{w}} + pV_{\mathrm{w}}}{RT}\right] \tag{2}$$

$$\eta_{\mathrm{Y}} = \frac{\sigma_{\mathrm{Y}}(p, C_{\mathrm{w}})}{2\,\dot{e}} \tag{3}$$

$$\sigma_{\mathrm{Y}}(p, C_{\mathrm{w}}) = C_{\mathrm{Y}} + \mu(C_{\mathrm{w}})p; \quad \mu(C_{\mathrm{w}}) = \min\left[1, \left(\frac{c_{\mathrm{w}}}{c_{\mathrm{w,ref}}}\right)^{-1}\right]\mu_0 \tag{4}$$

$$\eta = \left(\frac{1}{\eta_{\mathrm{d}}} + \frac{1}{\eta_{\mathrm{w}}} + \frac{1}{\eta_{\mathrm{Y}}}\right)^{-1} \tag{5}$$

where A_k is the prefactor determined by $T = 1600$ K at the surface (the subscript k indicates either 'd' for dry mantle or 'w' for hydrous mantle), E_k is the activation energy, V_k is the activation volume, C_{w} is the water content in the mantle, $C_{\mathrm{w,ref}}$ is the reference water content assumed to be 620 ppm, Γ_{ij} is the phase function, f_j is the basaltic composition, R is the gas constant, T is the temperature, p is the dynamic pressure, C_{Y} is the surface cohesion factor, μ is the friction coefficient as a function of the mantle water content, μ_0 is the friction coefficient of dry rock, and $\dot{e}$ is the second invariant strain rate tensor. It is noted that the subscripts of the viscosity i (up to 3) and j (up to 4) in Eqs. (1) and (2) represent the index of the phase transition from a deeper to a shallower transition (i.e. $i = j = 1$: post-perovskite phase boundary, $i = j = 2$: bridgmanite phase boundary, $i = 3$: olivine–spinel boundary, $j = 3$: pyroxene–garnet boundary, and $j = 4$: eclogite transition). Besides, we note that the water-dependent friction coefficient is assumed, which was simplified by Gerya et al. (2008), because, in our modeling approach of the mantle water cycle, it is difficult to compute the fluid pore pressure. Hence, the friction coefficient depends similarly on water since viscosity is water dependent. However, there are a few choices instead of water-weakening effects that may reduce the yield strength of oceanic lithosphere, for instance, the temperature effects incorporating the friction coefficient (Karato and Barbot, 2018) and grain-size reduction (e.g., Foley, 2018). Here, we select the water-

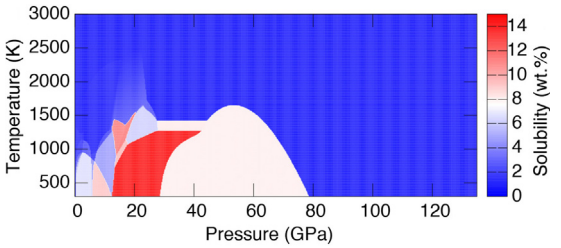

Fig. 1. Water solubility map of the ambient mantle material in the whole mantle pressure and temperature range. For the water solubility of the oceanic crust, we use the same solubility in the upper mantle as that proposed by Iwamori (2007), and we use that of the ambient mantle material in the lower mantle because of the similar mineral phases expected.

weakening effects to reduce the yield strength of ambient oceanic lithosphere.

To compute the thermo-chemical mantle convection, we use the StagYY numerical code for simulating thermo-chemical mantle convection (Trackley, 2008). Detailed information on the mantle convection simulations and water migration can be found in a series of our previous studies (Nakagawa and Iwamori, 2017; Nakagawa and Spiegelman, 2017; Nakagawa et al., 2015, 2018) and in the Appendix. The water solubility of hydrous mantle silicates is applied as in Nakagawa et al. (2018), including the water solubility of dense hydrous magnesium silicate (DHMS), as shown in Fig. 1, which is based on experimental data (Nishi et al., 2014; Ohira et al., 2014). Briefly described, when the water in the mantle material exceeds the assigned water solubility, the excess water can be generated from the difference between the actual water content in the mantle silicate and the water solubility of the hydrous mantle mineral. We also include a reduction of the solidus temperature of the mantle silicate according to the similar scaling law provided by Katz et al. (2003), and the partitioning of water into the molten mantle is assumed with a partition coefficient of 0.01 between the solid and molten mantle, which means that 99% of water is partitioned into the molten material. The numerical resolution of the mantle convection model is 1024×128 with 4 million tracers for tracking the chemical composition, melt fraction, and water content.

For the initial conditions of the mantle, the initial temperature profile is set with an adiabatic temperature of 2000 K at the surface, the mantle composition is uniform (20% basaltic material and 80% depleted harzburgitic material), and the water content is zero. The surface boundary condition is fixed as 300 K, but we use the energy of the core evolution described below at the CMB. For the boundary condition of mantle water circulation, a finite reservoir of surface seawater with a box model assumption is used. The mass of the water reservoir can be computed as

$$X_{\mathrm{w,s}} = X_{\mathrm{w,total}} - X_{\mathrm{w,m}}(F_{\mathrm{R}}, F_{\mathrm{H}}, F_{\mathrm{G}}) \tag{6}$$

where $X_{\mathrm{w,s}}$ is the mass of the water ocean, $X_{\mathrm{w,total}}$ is the mass of the total amount of water in the system and $X_{\mathrm{w,m}}$ is the mass of mantle water as a function of regassing (F_{R}), dehydration (F_{H}), and degassing (F_{G}). The boundary condition of mantle water migration at the surface is described as follows:

$$C_{\mathrm{w}}(\mathrm{surface}) = \begin{cases} C_{\mathrm{w,sol}}(300\mathrm{K}, \mathrm{surface}) \ \ if \ \ X_{\mathrm{w,s}} > 0 \\ 0 \ \ if \ \ X_{\mathrm{w,s}} = 0 \end{cases} \tag{7}$$

where $C_{\mathrm{w,sol}}$ (300 K, surface) is the water solubility of mantle rocks at the surface. For the hydration thickness, we assume 5 km. For the hydration process, it is assumed that tracers may have the amount of water shown in Eq. (7) when tracers come inside 5 km below the surface. This formulation means that water may be incorporated into the oceanic crust following an instantaneous process caused by hydrothermal alternation (e.g., Rüpke et al., 2004) or serpentinization in the outer-rise fault (Hatakeyama et al., 2017; Korenaga et al., 2017), but it is still very uncertain (Höning et al., 2014). Note that, in this study, we assume a fully-saturated situation of crustal hydration, but it seems not to be a water-saturated condition in the oceanic crust (e.g., Carlson, 2003) or a limited amount of water transport via pore fluid (Jarrard, 2003). Hence, in this study, we indicate the maximum estimate of water evolution expected in a coupled core–mantle evolution. However, results would not be changed if we used the hydrous situation at the surface, that is, the under-saturated condition of basaltic crust (See Appendix A4). The hydrated condition of the oceanic lithosphere means that the hydrous condition in the deep mantle could be determined by the storage capacity limit of hydrous mantle minerals. As indicated in the previous study (Nakagawa and Spiegelman, 2017), the major region in which the mantle water cycle is occurring is up to 150 km in depth, because a large amount of water may experience degassing and dehydration at that depth. This dehydration is caused by effects of water solubility maps of the mantle mineral, that is, by incorporating an effect of choke-point. Since the numerical model used in this study is a global-scale model, it would be difficult to resolve more detailed processes that may have happened in the subduction zone expected by geological and geochemical analysis (Bodnar et al., 2013; Maruyama and Okamoto, 2007).

With regard to the core evolution incorporated into the mantle convection simulations, the temperature at the CMB is computed from an energetic formulation based on Buffett et al. (1992) and Buffett et al. (1996) for the global heat balance and Lister (2003) for the entropy balance, which is similar to the implementation of Nakagawa and Tackley (2010), whose detailed formulation of core evolution is given in Appendix A3. A simplified and analytical formulation of the heat balance is assumed across the core, with uniform composition and an isentropic temperature due to well-mixed convective conditions for the core evolution. The initial CMB temperature is considered to be 5000 K, which is ~1500 K higher than the solidus temperature of silicates found in high-P–T experiments (e.g., Andrault et al., 2014; Nomura et al., 2014). This initial condition of the CMB temperature would be observed for a

Table 1
Mantle model physical parameters.

Symbol	Meaning	Value
η_0	Reference viscosity	1×10^{21} Pa s
ρ_0	Surface density	3300 kg m^{-3}
g	Surface gravity	9.8 m·s^{-2}
α_0	Surface thermal expansivity	5×10^{-5} K^{-1}
κ_0	Surface thermal diffusivity	7×10^{-7} m^2 s^{-1}
ΔT_{sa}	Temperature scale	2500 K
T_s	Surface temperature	300 K
C_p	Heat capacity	1250 J kg^{-1} K^{-1}
L_m	Latent heat	6.25×10^5 J kg^{-1}
H	Present-day internal heating rate	5×10^{-12} W kg^{-1}
λ	Half-life of radioactive elements	2.43×10^9 yr
C_Y	Cohesion stress	10 MPa
E_d	Activation energy of the dry mantle	290 kJ mol^{-1}
V_d	Activation volume of dry mantle	2.4×10^{-6} m^3 mol^{-1}
E_w	Activation energy of wet mantle	380 kJ mol^{-1}
V_w	Activation volume of wet mantle	4×10^{-6} m^3 mol^{-1}

The activation energy and dry mantle volume are from Yamazaki and Karato (2001), and those for the wet mantle are from the wet rheology of olivine (Korenaga and Karato, 2008). The latent heat caused by partial melting is taken from Xie and Tackley (2004).

partial melting region in the deep mantle coincident with a basal magma ocean (Labrosse et al., 2007).

All physical parameters used in this study are listed in Table 1 for the mantle and Table 2 for core evolution.

2. Results

A total of six cases are examined to investigate how hydrous mantle convection affects core evolution. The total amount of water in the entire planetary system is assumed as the control parameter of this study, which varies from 3 to 15 ocean masses (i.e. with a present-day ocean mass of 1.4×10^{21} kg). All cases are set for a friction coefficient of 0.3. This friction coefficient is a nearly lower-bound value of the observational constraints on the strength of the oceanic lithosphere, and is in the range from 0.2 to 0.7 (Zhong and Watts, 2013).

Table 2
Physical parameters for the core evolution model. The theoretical model of core evolution energies is based on Buffett et al. (1992) and Buffett et al. (1996), with some modifications for computing the latent heat release caused by inner core growth.

Symbol	Meaning	Value
ρ_0	Density at the center	12491 kg m^{-3}
c_p	Heat capacity	750 J kg^{-1} K^{-1}
$T_{m,0}$	Melting temperature at the center	4900 K
g	Gravity	9.8 m s^{-2}
G	Gravitational constant	6.67×10^{-11} m^3 kg^{-1} s^2
$(\partial T_L/\partial P)_X$	Pressure derivative	9×10^{-9} K Pa^{-1}
$(\partial T_L/\partial X)_P$	Composition derivative	-2.04×10^4 K
k_c	Thermal conductivity	100 W m^{-1} K^{-1}
γ	Grüneisen parameter	1.4
ΔS	Entropy change	118 J kg^{-1}
$\Delta\rho_{IC}$	Density change due to inner core growth	580 kg m^{-3}
R	Gas constant	8.314 J K^{-1} mol^{-1}
$X_{m,0}$	Initial concentration of light elements	0.05

2.1. Dry vs. hydrous

First, to discuss how hydrous mantle convection affects the core–mantle evolution system, Fig. 2 shows the chemical-viscous-hydrous structure taken at 4.6 billion years from the initial conditions. For the case of hydrous mantle convection, we use six ocean masses as a total water mass in the planetary system. The dry mantle model seems to exhibit episodic plate-like behavior; as a result, flat layering above the CMB region can be found. Meanwhile, vigorous plate-like behavior is observed for the hydrous mantle convection model owing to the water-weakening effect, and the model contains four large subduction regions with small-scale compositional anomalies in the deep mantle. This means that the water-weakening effect may enhance surface plate motions, as was noted by Nakagawa and Iwamori (2017). Also, the high-water-content region in subducting slabs can penetrate the uppermost lower mantle corresponding to the substantial water solubility associated with DHMS (e.g., phase D).

Fig. 3 shows comparisons of the core evolution diagnostics between the dry and hydrous mantle models. The heat flow across the CMB is higher for hydrous mantle convection than for dry mantle convection, which is attributable to a difference in the mode of surface plate motion. As a result, the CMB heat flux seems to be very small for the dry mantle model, but it reaches 10 TW for hydrous mantle convection.

2.2. Sensitivity of the total water amount in the planetary system

Fig. 4 shows the chemical-viscous-hydrous structure taken at 4.6 billion years for a total water amount of 6 and 15 ocean masses in the planetary system. Compared to the hydrous mantle convection model (left of Fig. 4; 6 ocean masses with stronger oceanic lithosphere) with that shown in the right side of Fig. 2 (6 ocean masses with weak oceanic lithosphere), the plate-like behavior displayed in the left side of Fig. 4 is slightly less vigorous because of the high friction coefficient used in those cases. As a result of the less vigorous plate-like behavior, compositional anomalies at larger scales in the deep mantle are likely to be preserved. Concerning the mantle water content, large amounts of water are found in the uppermost lower mantle region beneath cold subduction regions. Again, as suggested by Nakagawa et al. (2018), this is caused by the appearance and dissolution reaction of phase D.

Fig. 5 plots the amounts of surface seawater and mantle water and the mass-averaged mantle temperature as a function of time for all hydrous mantle convection cases, and the 1-D horizontally-averaged water content and temperature taken at 4.6 billion years for a total water amount of 15 ocean masses. Up to the case of 12 ocean masses, the surface ocean is completely transported into the deep mantle within 4.6 billion years; for the case with 15 ocean masses, the surface ocean may survive over 4.6 billion years. Therefore, for the cases between 12 and 15 ocean masses, the present-day Earth could have one ocean mass at the surface. Note that this is a maximum

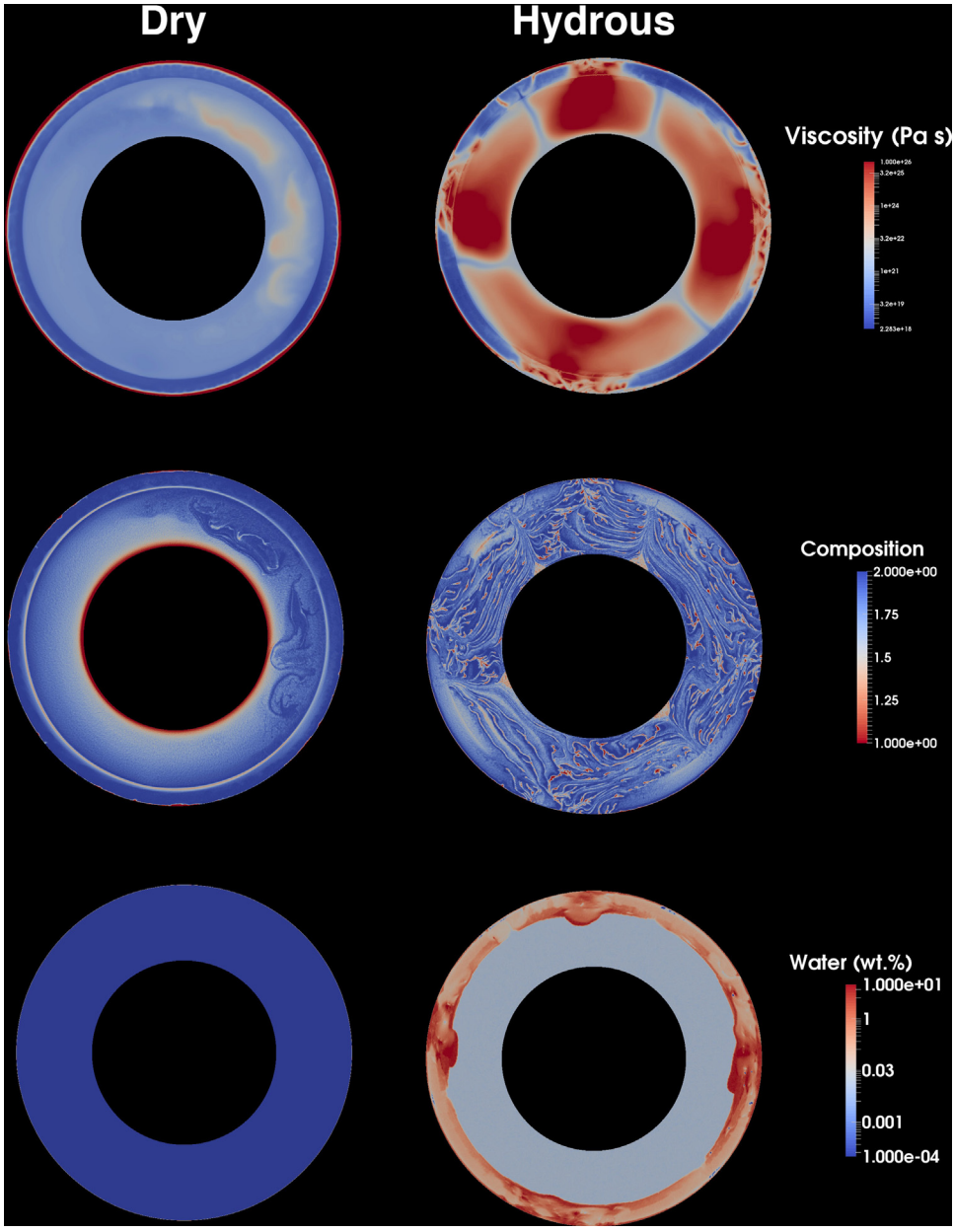

Fig. 2. Viscous-chemical-hydrous structure taken at 4.6 billion years for the dry (left) and hydrous (right) mantle convection simulations.

estimate. Regarding the estimates of the total water mass in the mantle reported by Iwamori (2007), the mantle may have absorbed approximately ∼12 ocean masses at the maximum estimate, which is consistent with the ocean masses expected in this study. However, note that this maximum estimate of the water mass of the mantle is computed in the saturated situation for oceanic lithosphere, but an experimental constraint on the water content of oceanic crust suggests that the oceanic crust would be in the undersaturated condition (e.g., Carlson, 2003). Preferably, the mantle water mass would be ∼6 to 7 ocean masses indicated in the averaged value of mantle water mass (Table 3 in Iwamori, 2007). Theoretical model on partitioning of hydrogen in the mantle silicate at lower mantle condition is also indicated as the similar value (Table 2 in Merli et al., 2016). In Fig. 5b, the mantle water contents at depths above the first 200 km and between the depths of 700 km and 900 km are computed as approximately 4.2 and two ocean masses, respectively. For understanding why a large amount of water can be transported into such regions, the relationship of mantle temperature and water solubility is a key. Fig. 5c shows the 1-D horizontally-averaged mantle temperature. Since the cold geotherm may pass through below the choke-point of water solubility maps (see Fig. 1), a large amount of water can be transported into the mantle transition zone as well

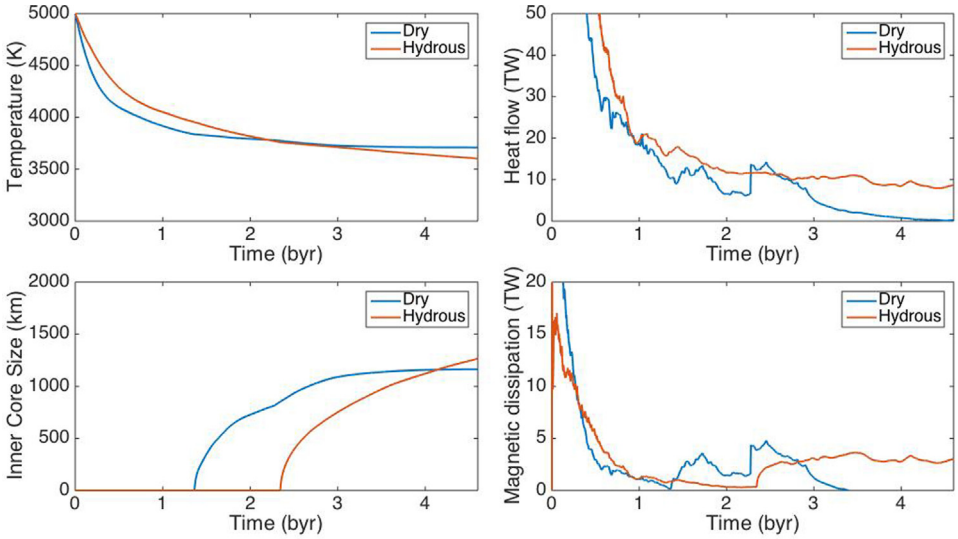

Fig. 3. Evolution diagnostics (temperature at the CMB, heat flow across the CMB, inner core size and magnetic dissipation) of the core for the dry and hydrous mantle convection cases.

as into the uppermost lower mantle associated with the high-solubility region caused by DHMS. This suggests that the cold downwelling flow can work for the main host of water transporting into the deep mantle. Again, note that an actual water mass absorbed in the mantle would be less than this estimate, because the hydrous condition in the oceanic lithosphere would be undersaturated to give a value of the water mass of the mantle consistent with the expected averaged values of Iwamori (2007) and Merli et al. (2016).

Fig. 6 shows the mantle water fluxes (ingassing, dehydration and degassing) as a function of time for the cases with six ocean masses (all surface water is transported into the deep interior) and 15 ocean masses (surface water remains on the surface). The computing procedures are found in Nakagawa and Spiegelman (2017) and Nakagawa et al. (2018). The detailed description can be found in Appendix A2.

Fig. 7 shows the sensitivity of core evolution for all cases of convection of the hydrous mantle. There is less sensitivity in core evolution with different choices of the total amount of water in the planetary system. On the present-day Earth, the temperature at the CMB is estimated to be ∼3600 K, and the heat flow across the CMB is 10 TW; the inner core is 2 billion years old, and continuous dynamo activity has lasted over 4 billion years, as obtained from this numerical model. These values seem to be similar to a series of previous studies for dry mantle convection with weaker plate cases (e.g., Nakagawa et al., 2010). For the CMB heat flow, it would be in the range 5–15 TW (e.g., Lay et al., 2008). For the age of the inner core, it would be older than recent results that evidence a much younger inner core (e.g., Biggin et al., 2009), but it would be still very controversial because the paleomagnetic data for constraining the age of the inner core would suffer a huge discrepancy. As discussed in the previous sections, hydrous mantle convection would be more promising for revealing the evolution of the core–mantle–plate–ocean system that matches various observational constraints (i.e. the geomagnetic field, the size of the inner core, and the current amount of surface seawater).

Regarding the heat flow across the CMB and the age of the inner core, various theoretical studies on core evolution and paleomagnetism suggested much higher heat flow values and younger inner core ages (Biggin et al., 2009; Davies, 2015; Labrosse, 2015). However, in particular, the paleomagnetic data that could be utilized to imply the age of the inner core still seems to be controversial due to uncertainties in the data (Biggin et al., 2009).

3. Discussion and summary

3.1. Findings

Here, we investigate the effects of hydrous mantle convection on the evolution of the core. Moreover, we also discuss the evolution of surface seawater by providing a constraint on the amount of water that has been delivered since the early planetary formation. The main findings in this study are as follows.

Hydrous mantle convection is a crucial process for understanding the cooling processes of the core–mantle system caused by the viscosity reductions occurring under the effect of water-dependent viscosity.

To accommodate one ocean mass for the present-day Earth, the total amount of water in the planetary system was between 12 and 15 ocean masses at the maximum. This seems to be consistent with the maximum water mass in the mantle found from a realistic geotherm (Iwamori, 2007). However, more preferably, the mantle water mass could be absorbed in ∼6 to 7 ocean masses (averaged value in Table 3 in Iwamori, 2007; Table 2 in Merli et al., 2016). This suggests that the hydration condition of the oceanic lithosphere would not be saturated, which is pointed out by an experimental constraint of water content in the

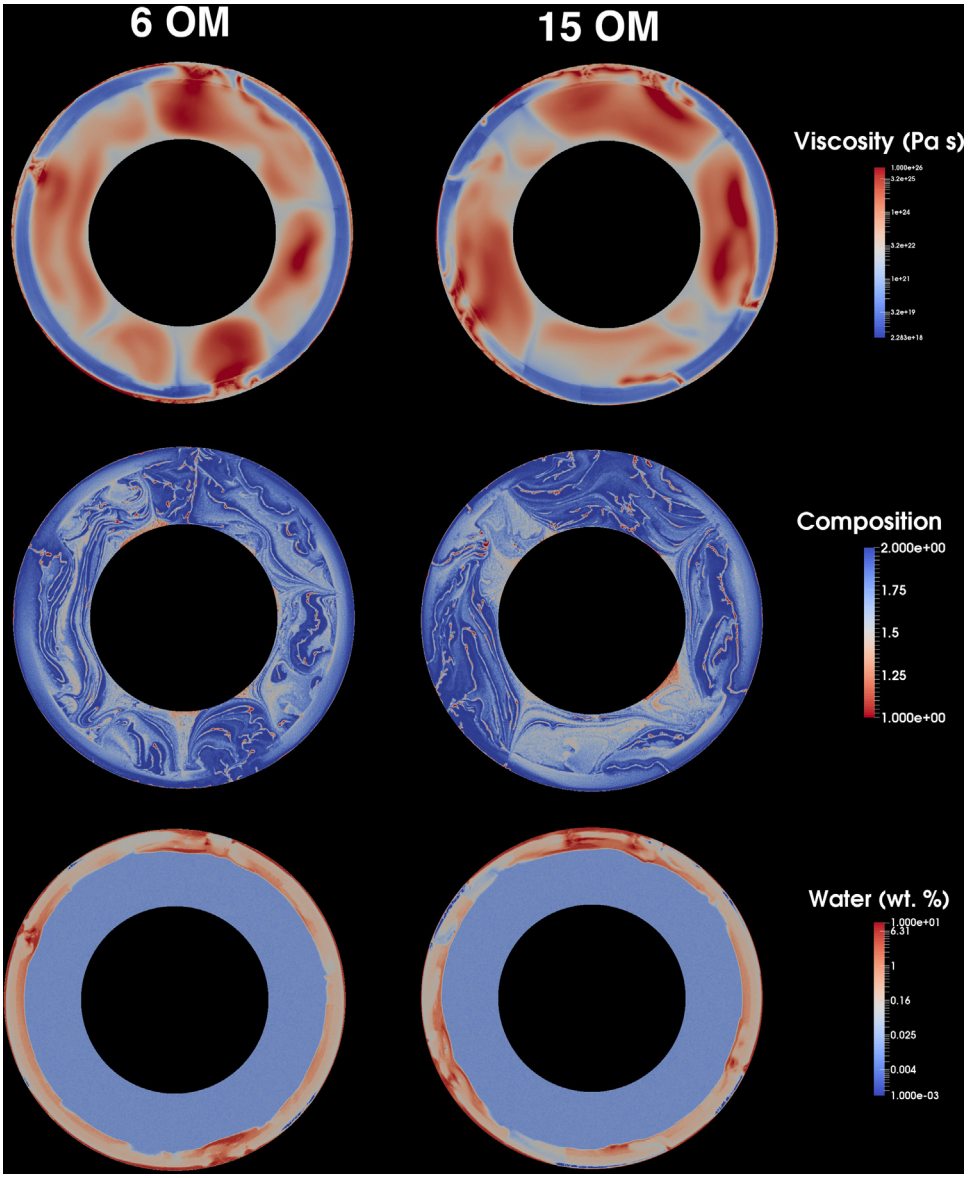

Fig. 4. Viscous-chemical-hydrous structure taken at 4.6 billion years for total water amounts of 6 OM in the planetary system (left) and 15 OM (right).

oceanic crust (e.g., Carlson, 2003). As discussed in the Appendix A4, the hydration condition of the oceanic crust may not be very sensitive, and the storage capacity of water in the mantle mineral may be determined for the hydration situation in the deep mantle. In the subduction-scale modeling, the minimum water content of oceanic lithosphere may be around two wt. percent to generate the volcanic activities beneath the island arc (Horiuchi and Iwamori, 2016). Therefore, this modeling result seems to be somewhat robust to discuss the Earth-like features of the mantle water cycle.

This is the first attempt to develop a coupled evolutionary model for the core–mantle–plate–ocean system. Although core evolution in hydrous mantle convection is not very sensitive to the total amount of water in the planetary system, the hydrous models explain the heat flux across CMB better compared to the dry model.

3.2. A total amount of water in the planetary system

As discussed in the previous section, the mantle water mass studied here is consistent with the maximum estimate of the water mass of the mantle using the realistic geotherm (Iwamori, 2007). However, more preferably, the mantle water mass could be absorbed in ∼6 to 7 ocean masses with water solubility and partitioning of hydrogen (averaged value shown in Table 3 of Iwamori (2007); Table 2 of Merli et al. (2016)). For estimating the maximum amount of mantle water mass, this is based on the saturated condition in the oceanic lithosphere and uppermost lower

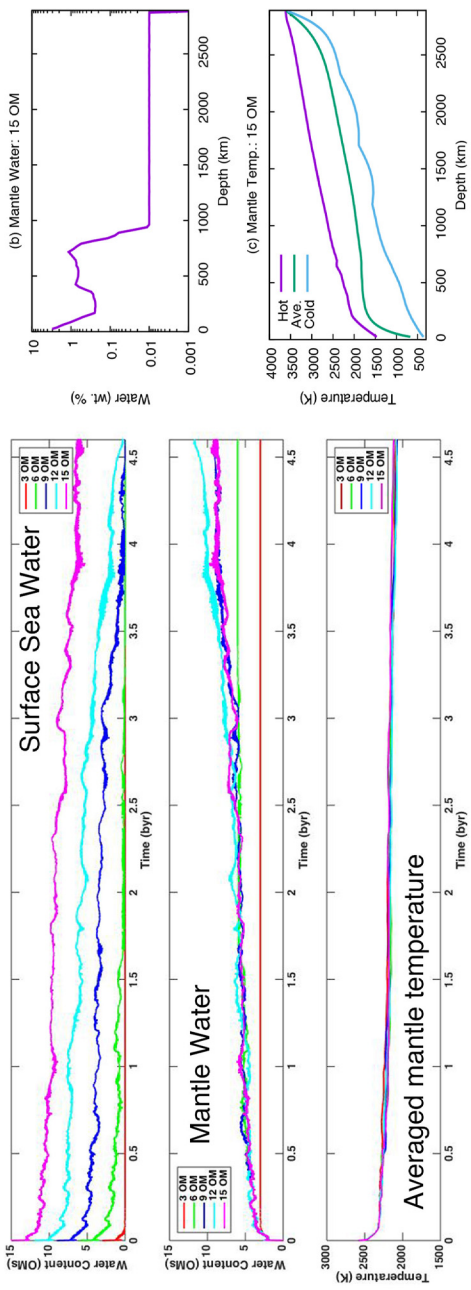

Fig. 5. (a) Evolution diagnostics of the surface water mass (top), mantle water mass (middle), and mantle temperature (bottom) for each value of the total water amount in the planetary system. (b) 1-D horizontally-averaged profile of the mantle water content for 15 OM and (c) 1-D horizontally-averaged profile of the mantle temperature for 15 OM.

mantle. As shown in Fig. 5b and c, the oceanic lithosphere seems to be the water-saturated situation. Therefore, our estimate of the absorbed water in the mantle is similar to the maximum one proposed by Iwamori (2007). However, the water content in the oceanic crust ranging from 0.5 to 6 wt. % is found from experimental estimates (Aubaud et al., 2008; Carlson, 2003), which is considerably uncertain, but suggests that the hydrous situation of oceanic crust may be undersaturated for the water.

Moreover, the heterogeneous condition of hydration of oceanic crust caused by thermal cracking phenomena (Korenaga, 2007) and serpentinization in the outer-rise fault (Hatakeyama et al., 2017) should be incorporated for further understanding of the transport of water into the deep mantle and of the hydrous structure in the deep mantle. Again, in our model, the boundary condition of mantle water transport is assumed with the water-saturated condition of oceanic crust. To check how the hydrous situation of oceanic crust affects the results, as indicated in Appendix A4, we evaluate the sensitivity of the water content of oceanic lithosphere to water evolution. As a result, the evolution diagnostics of water in both mantle and surface are not strongly sensitive to the hydration condition of the oceanic lithosphere, even though it is the undersaturated condition. As a result, the storage capacity of water in mantle minerals could play a more key role in the hydration condition in the deep mantle than the hydration condition of oceanic crust. Any hydration mechanism could result in a similar evolution scenario. However, again, we note that this estimate of water evolution is still the maximum one; the result might be changed if the water solubility limit of hydrous mantle minerals were revised, but the current understanding of the storage capacity of water suggests that the results shown in this study are still robust. Also, the sensitivity of the power-law index of the water-dependent viscosity should be tested because a recent experimental investigation suggested that this index should be $r = 0.3$ (Fei et al., 2013), which is much lower than that used in this study ($r = 1.0$).

There are several caveats before interpreting numerical results. For the evolution of surface seawater, other studies would indicate a different scenario provided from geochemical and geological accomplishments, that is, 'continental freeboard' (Korenaga et al., 2017; Parai and Mukhopadhyay, 2012) and D/H ratio evolution of the Archean seawater (Kurokawa et al., 2018). In these authors' implications, the mantle water mass would not be very large, likely 1 to 2 ocean masses. However, these studies have not incorporated the effects of water solubility of each mantle minerals for evaluating the evolution of the water mass of the mantle. Hence, the present-day mantle water mass would be still controversial. For resolving this issue, it would be required to check the numerical model of hydrous mantle convection rather than to use a simple mass flux computation without assuming the solubility of water in each mantle mineral.

Regarding the sea level change inferred from the continental freeboard hypothesis, this would not be changed over a time scale of a few billion years (~500 m; Korenaga et al., 2017; Parai and Mukhopadhyay, 2012). This implies

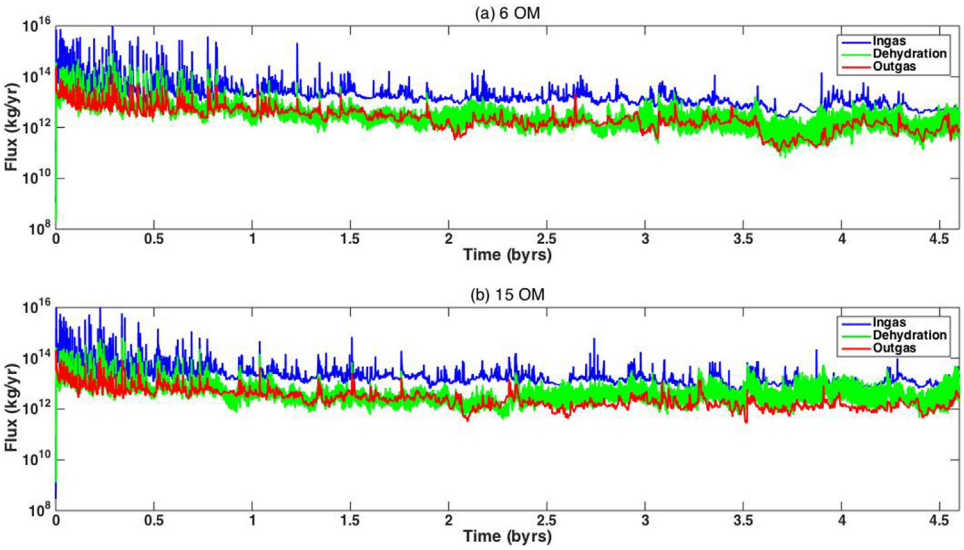

Fig. 6. Diagnostics of the water fluxes (ingassing: blue, degassing: red and dehydration: green) for (a) 6 OM and (b) 15 OM.

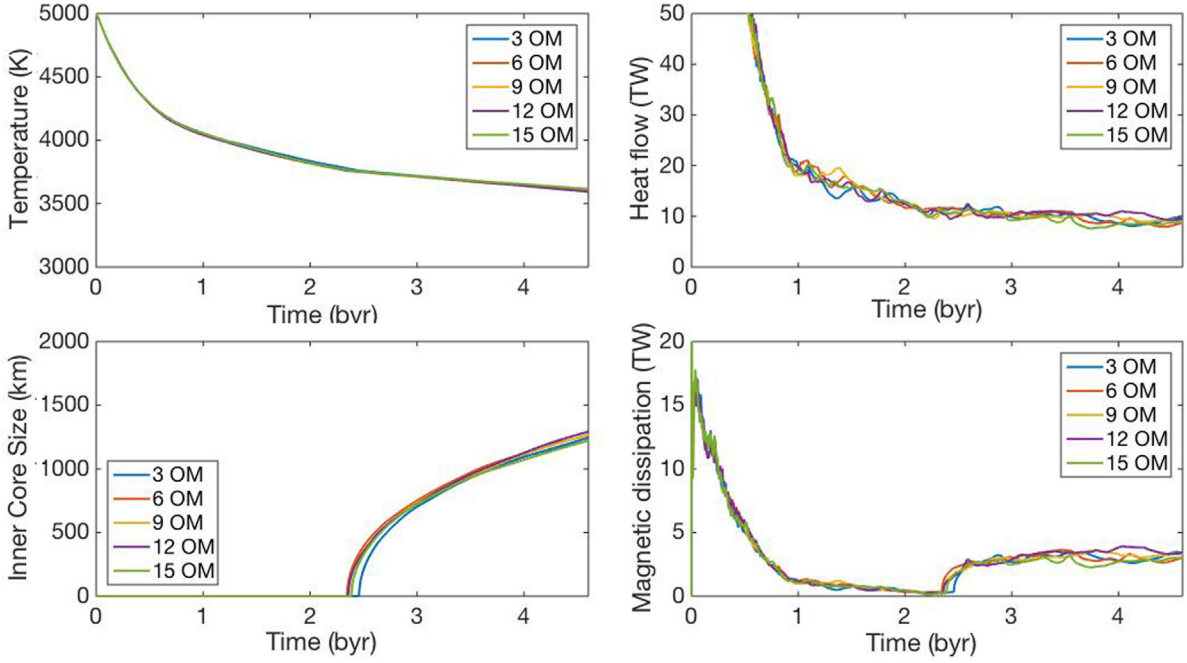

Fig. 7. Model sensitivities of the core evolution diagnostics to each amount of the total water in the planetary system.

that the water budget between the deep Earth and the exosphere would have been balanced for over a few billion years. As pointed out by the potential water mass in the deep mantle inferred from the water solubility limit of mantle minerals, the mantle may have 6 to 8 ocean masses (Iwamori, 2007). This suggests that the mantle may have a huge amount of water in the early state of the Earth. To have a huge amount of water in deep mantle, looking at Fig. 1, the temperature in the early mantle of the Earth should be much colder than assumed in this study, because the water content in the mantle is strongly regulated by the water solubility limits (Nakagawa and Spiegelman, 2017). For the thermal state from the early mantle to the present-day mantle, a situation similar to that proposed by Korenaga (2011) would be somewhat expected, which may start with colder temperatures in the mantle, which would be heated up by a heat-producing element, then cooled down by vigorous mantle convection. However, note that, in this study, the continental lithosphere is not included in the numerical model; this argument is still quite speculative. To tackle the issue on the free-board hypothesis and other important processes such as the

formation of sediments, it is a crucial issue that should be addressed more systematically in numerical modeling of mantle convection, which has been initiated for the generation of the precursor material of the continental crust (Rozel et al., 2017). In this study, we have started with the development of the thermal and chemical history of hydrous mantle convection, then addressing the formation of continental crust for discussing the free-board hypothesis in the future study.

Moreover, regarding estimates of water flux associated with subduction, it would be less by a few orders of magnitude than our estimate shown in Fig. 6 (Bodnar et al., 2013; Jarrard, 2003). In Fig. 6, we computed the ingassing flux across the surface. Assuming the effects of the chokepoint of solubility of the water content in the mantle, the ingassing flux associated with subduction would be reduced up to three orders of magnitude of the ingassing flux across the surface (Nakagawa et al., 2015). This means that the actual water flux transported into deep mantle would be an amount similar to the recent estimate of the water flux. Therefore, simplified arguments on mantle water flux are still very controversial, but the actual water mass in the mantle could not be estimated from the mass balance assumption.

3.3. Implications for water transport across the core–mantle boundary: hydrogen partitioning

As suggested from high-temperature and high-pressure mineral physics, hydrogen may be generated by the reaction of water with iron-bearing minerals during lower mantle convection (Hu et al., 2016; Nishi et al., 2017). Since hydrogen seems to be one of the most important light elements in core alloys (Poirier, 1994), understanding the amount of hydrogen that can be transported via the metal–silicate partitioning of hydrogen into metallic iron seems to be significant. Unfortunately, there has been quite few publications that addressed the metal–silicate partitioning of hydrogen into metallic iron, and this partitioning occurred at relatively lower pressure and temperature (e.g., Okuchi, 1997). An implication of the partitioning of hydrogen in core alloys suggests, when extrapolating such an experimental constraint to the conditions in the deep mantle, that hydrogen seems to be partitioned into metallic iron and that it never returns to the silicate mantle. This suggests that hydrogen is generated at the lower mantle condition associated with the water absorbed in the lower mantle. The metal–silicate partitioning of hydrogen can result in hydrogen transportation into the metallic core. Therefore, the hydration state of the lower mantle plays a key role for the partitioning of hydrogen into the metallic core caused by metal–silicate partitioning. However, recent investigations on metal–silicate partitioning of hydrogen between metallic core and silicate mantle indicate that hydrogen is likely to be partitioned into the silicate mantle (Clesi et al., 2018). The hydrogen in the Earth's core might be trapped as a result of metal–silicate partitioning due to core formation in the early Earth (Iizuka-Oku et al., 2017). This may suggest that the hydrous conditions in the deep mantle could be expected as the large-scale anomalies caused by thermal and chemical effects.

To further clarify that, investigations of the metal–silicate partitioning of hydrogen should be conducted in greater detail to integrate the water cycle into the core–mantle–plate–ocean system completely, which may reveal the hydration state in the lower mantle. It has to be noted that this type of metal–silicate partitioning could occur through the interaction with the silicate melt. The melting temperature of the silicate mantle ranges from 3500 K to 3800 K (Andrault et al., 2014; Nomura et al., 2014). Compared with the temperature at the CMB found in this study, that is, a present-day temperature of ∼3600 K, the metal–silicate partitioning of hydrogen could have occurred from a few billion years ago to the present day (when the melting temperature would be at a minimum). However, it would have stopped in a couple of billion years at a maximum value of the melting temperature at the CMB (see Fig. 7). This suggests that the survival time of a basal magma ocean would play a key role in operating such a metal–silicate partitioning process. However, again, the hydrogen of the Earth's core is still quite a controversial issue. For resolving that, more investigations are needed.

4. Conclusion

In this study, we developed a core–mantle–plate–ocean evolution model through a numerical mantle convection simulation. The findings can be summarized as follows.

To understand the long-term evolution of the Earth and of the planetary system, hydrous mantle convection is an essential process for a successful scenario describing core evolution, because hydrous mantle convection may enhance the heat transfer associated with mantle convection, with viscosity reductions caused by water-dependent viscosity.

The present-day amount of surface seawater within the mantle dynamics system would require between 12 and 15 ocean masses in the total planetary system. This means that the deep planetary interior may contain more than ten ocean masses. This also constitutes an enormous amount of water that has been absorbed into the mantle compared to values from a series of previous modeling studies on the mantle water cycle (Rüpke et al., 2004; Sandu et al., 2011). As incorporated into the water solubility map in the numerical mantle convection simulation, the water transported into the deep mantle seems to be mainly absorbed into the mantle transition zone and DHMS phases that have a solubility of ∼10%. However, considering a realistic geotherm with a temperature that is higher by a few hundred kelvins than the thermal structure in this study, this may suggest that DHMS solubility would not be significant for a contribution to the mantle water mass. Therefore, the mantle water mass is likely reduced to 6–7 ocean masses (Iwamori, 2007; Merli et al., 2016). However, since there is another hypothesis on the effects of the buoyancy of continental lithosphere that is not incorporated into this study, the amount of water in the deep mantle is still controversial.

Our findings imply that the partitioning of hydrogen could supply the partitioning of hydrogen associated with water absorbed into lower mantle minerals caused by metal–silicate partitioning into metallic iron. However, as

suggested from experimental constraints (Clesi et al., 2018; Iizuka-Oku et al., 2017), partitioned hydrogen seems to be difficult to occur over the Earth's history, which might result in the differentiation of the core formation process in the early Earth. For more clarifying the hydrogen cycle in the whole planetary system, it would be worth to integrate the global-scale water cycle into the core–mantle–plate–ocean system based on the numerical model used in this study.

Acknowledgments

The authors thank Atsushi Nakao for the water solubility of the DHMS phases incorporated into the numerical mantle convection simulations and Paul Tackley for providing his numerical mantle convection code (StagYY). They also thank two anonymous reviewers for improving the original manuscript significantly. All of the simulation data are available from the corresponding author (TN) upon request, but the numerical simulation program is the property of the developer (Paul Tackley), and the water solubility data are the property of HI and are not available to the public. JSPS-MEXT Kakenhi financially supports TN through the 'Core–mantle Co-evolution' (15H05834), JSPS Kahenhi (JP16K05547), the FLAGSHIP2020 project, and MEXT within the CBSM2 project "Structure and Properties of Materials in the Deep Earth and Planets." All numerical simulations were performed under the JAMSTEC Data Analyzer system.

Appendix A. Supplementary data

Supplementary data associated with this article can be found, in the online version, at https://doi.org/10.1016/j.crte.2019.02.001.

References

Andrault, D., Pesce, G., Ali Bouhifd, M., Bolfan-Casanova, N., Hénot, J.-M., Mezouar, M., 2014. Melting of subducted basalt at the core–mantle boundary. Science 344, 892–895, http://dx.doi.org/10.1126/science.1250466.

Aubaud, C., Hirschmann, M.H., Withers, A.C., Hervig, R.L., 2008. Hydrogen partitioning between melt, clinopyroxene, and garnet at 3 GPa in a hydrous MORB with 6 wt, % H2O. Contrib. Mineral. Petrol. 156, 607–625.

Biggin, A.J., Strik, G.H.M.A., Langereis, C.G., 2009. The intensity of the geomagnetic field in LateArchean: New measurements and an analysis of the updated IAGA paleointensity database. Earth Planet. Space 61, 9–22.

Bodnar, R.J., Azbej, T., Becker, S.P., Cannatelli, C., Fall, A., Severs, M.J., 2013. Whole mantle geohydrologic cycle, from the clouds to the core: The distribution of water in the dynamic Earth system. The Geological Society of America Special Paper 500, 431–461.

Buffett, B.A., Huppert, H.E., Lister, J.R., Woods, A.W., 1992. Analytical model for solidification of the Earth's core. Nature 356, 329–331.

Buffett, B.A., Huppert, H.E., Lister, J.R., Woods, A.W., 1996. On the thermal evolution of the Earth's core. J. Geophys. Res. 101, 7989–8006, http://dx.doi.org/10.1029/95JB03539.

Carlson, R.L., 2003. Bound water content of lower oceanic crust estimated from model analysis and seismic velocities of ocean diabase and gabbro. Geophys. Res. Lett. 30, 2142, http://dx.doi.org/10.1029/2003GL018213.

Clesi, V., Buohifd, M.A., Bolfan-Casanova, N., Manthilake, G., Schiavi, F., Raepsaet, C., Bureau, H., Khodja, H., Andrault, D., 2018. Low Hydrogen contents in the cores of terrestrial planets. Science Adv. 4, e1701816, http://dx.doi.org/10.1126/sciadv.1701876.

Davies, C.J., 2015. Cooling history of Earth's core with high thermal conductivity. Phys. Earth Planet. Inter. 247, 65–79.

Fei, H., Wiedenback, M., Yamazaki, D., Katsura, T., 2013. Small effect of water on upper-mantle rheology based on silicon self-diffusion coefficients. Nature 498, 213–215, http://dx.doi.org/10.1038/nature12193.

Foley, B.J., 2018. The dependence of planetary tectonics on mantle thermal state: applications to early Earth evolution. Phil. Trans. R. Soc. A 376,, http://dx.doi.org/10.1098/rsta/2017.0409 20170409.

Genda, H., 2016. Origin of Earth's oceans: An assessment of the total amount history and supply of water. Geochem. J. 50, 27–42.

Gerya, T.J., Connolly, A.D., Yuen, D.A., 2008. Why terrestrial subduction one-sided? Geology 36, 43–46, http://dx.doi.org/10.1130/G24060A.1.

Hatakeyama, K., Katayama, I., Hirauchi, K., Michibayashi, K., 2017. Mantle hydration along outer-rise faults inferred from serpentinite permeability. Sci. Rep. 7, 13870, http://dx.doi.org/10.1038/s41598-017-14309.

Höning, D., Hansen-Goos, H., Airo, A., Sphon, T., 2014. Biotic vs. abiotic Earth: A model for mantle hydration and continental coverage. Planet. Space Sci. 98, 5–13.

Horiuchi, S., Iwamori, H., 2016. A consistent model for fluid distribution, viscosity distribution, and flow-thermal structure in subduction zone. J. Geophys. Res. Solid Earth 121, 3238–3260.

Hu, Q., Kim, D.Y., Yang, W., Yang, L., Meng, Y., Zhang, L., Mao, H.-K., 2016. FeO_2 and FeOOH under deep lower-mantle conditions and Earth's oxygen-hydrogen cycles. Nature 534, 241–244, http://dx.doi.org/10.1038/nature18018.

Iizuka-Oku, R., Yagi, T., Gotou, H., Okuchi, T., Hattori, T., Sano-Furukawa, A., 2017. Hydrogeneration of iron in the early stage of Earth's evolution. Nat. Commun. 8, 14096, http://dx.doi.org/10.1038/ncomms14096.

Iwamori, H., 2007. Transportation of H_2O beneath the Japan arcs and its implications for global water circulation. Chem. Geol. 239, 182–198.

Jarrard, R.D., 2003. Subduction fluxes of water, carbon dioxide, chlorine, and potassium. Geochem. Geophys. Geosyst. 4 , http://dx.doi.org/10.1029/2002GC000392.

Karato, S.-I., 2011. Water distribution across the mantle transition zone and its implications for global material circulation. Earth. Planet. Sci. Lett. 301, 413–423, http://dx.doi.org/10.1016/j.epsl.2010.11.038.

Karato, S., Barbot, S., 2018. Dynamics of fault motion and the origin of constraining tectonic style between Earth and Venus. Sci. Reports 8, 11884, http://dx.doi.org/10.1038/s41598-018-30174-6.

Katz, R.F., Spiegelman, M., Langmuir, C.H., 2003. A new parameterization of hydrous mantle melting. Geochem. Geophys. Geosyst. 4, 1073, http://dx.doi.org/10.1029/2002GC000433.

Korenaga, J., 2007. Thermal cracking and the deep hydration of oceanic lithosphere: A key to the generation of plate tectonics? J. Geophys. Res. 112, B05408, http://dx.doi.org/10.1029/2006JB004502.

Korenaga, J., 2011. Thermal evolution with a hydrating mantle and the initiation of plate tectonics in the early Earth. J. Geophys. Res. 116, B12403, http://dx.doi.org/10.1029/2011JB008410.

Korenaga, J., Karato, S.-I., 2008. A new Analysis of experimental on olivine rheology. J. Geophys. Res. 113, B02403, http://dx.doi.org/10.1029/2007JB005100.

Korenaga, J., Planavsky, N.J., Evans, D.A., 2017. Global water cycle and the coevolution of the Earth's interior and surface environment. Phil. Trans. R. Soc. A375, 20150393, http://dx.doi.org/10.1098/rsta.2015.0393.

Kurokawa, H., Foriel, J., Laneuville, M., Houser, C., Usui, T., 2018. Subduction and atmospheric escape of Earth's seawater constrained by hydrogen isotopes. Earth Planet. Sci. Lett. 497, 149–160.

Labrosse, S., 2015. Thermal evolution of the core with a high thermal conductivity. Phys. Earth Planet. Inter. 247, 36–55.

Labrosse, S., Hernlund, J.W., Coltice, N., 2007. A crystallizing dense magma ocean at the base of the Earth's mantle. Nature 450, 866–869, http://dx.doi.org/10.1038/nature06335.

Lay, T., Hernlund, J., Buffett, B.A., 2008. Core–mantle boundary heat flow. Nature Geosci. 1, 25–32.

Lister, J.R., 2003. Expressions for the dissipation drive by convection in the Earth's core. Phys. Earth Planet. Inter. 140, 145–158.

Maruyama, S., Okamoto, K., 2007. Water transportation from the subducting slab into the mantle transition zone. Gondwana Res. 11, 148–165.

Merli, M., Bonadiman, C., Diella, V., Pavese, A., 2016. Lower mantle hydrogen partitioning between periclase and perovskite: A quantum chemical modeling. Geochim. Cosmochim. Acta 173, 304–318, http://dx.doi.org/10.1016/j.gca.2015.10.025.

Nakagawa, T., Iwamori, H., 2017. Long-term stability of plate-like behavior caused by hydrous mantle convection and water. Geophys. Res. 122 , http://dx.doi.org/10.1002/2017JB015052.

Nakagawa, T., Spiegelman, M.W., 2017. Global-scale water circulation in the Earth's mantle: Implications for the mantle water budget in the early Earth. Earth. Planet. Sci. Lett. 464, 189–199, http://dx.doi.org/10.1016/j.epsl.2017.02.010.

Nakagawa, T., Tackley, P.J., Deschamps, F., Connolly, A.D., 2010. The Influence of MORB and Harzburgite Composition on Thermo-Chemical Mantle Convection in a 3-D Spherical Shell With Self-Consistently Calculated Mineral Physics. Earth Planet. Sci. Lett 296, 403–412, http://dx.doi.org/10.1016/j.epsl.2010.05.026.

Nakagawa, T., Nakakuki, T., Iwamori, H., 2015. Water circulation and global mantle dynamics: Insight from numerical modeling. Geochem. Geophys. Geosyst. 16, 1449–1464, http://dx.doi.org/10.1002/2014/GC005701.

Nakagawa, T., Iwamori, H., Yanagi, R., Nakao, A., 2018. On the evolution of the water ocean in the plate–mantle system. Prog. Earth Planet. Sci. 5, 51, http://dx.doi.org/10.1186/s40645-018-0209-2.

Nishi, M., Irifune, T., Tsuchiya, J., Tange, Y., Nishihara, Y., Fujino, K., Higo, Y., 2014. Stability of hydrous silicate at high pressures and water transport to the deep lower mantle. Nature Geosci. 224–227, http://dx.doi.org/10.1038/NGEO2074.

Nishi, M., Kuwayama, Y., Tsuchiya, J., Tsuchiya, T., 2017. The pyrite-type high-pressure form of FeOOH. Nature 547, 205–208, http://dx.doi.org/10.1038/nature22823.

Nomura, R., Hirose, K., Uesugi, K., Ohishi, Y., Tsuchiyama, A., Miyake, A., Ueno, Y., 2014. Low core–mantle boundary temperature inferred from the solidus of pyrolite. Science 343, 522–525, http://dx.doi.org/10.1126/scince.1248186.

Ohira, I., Ohtani, E., Sakai, T., Miyahara, M., Hirao, N., Ohishi, Y., Nishijima, M., 2014. Stability of a hydrous δ-phase, AlOOH–$MgSiO_2(OH)_2$, and a mechanism for water transport into the base of lower mantle. Earth Planet. Sci. Lett. 401, 12–17, http://dx.doi.org/10.1016/j.epsl.05.059.

Okuchi, T., 1997. Hydrogen partitioning into molten iron at high pressure: Implications for Earth's core. Science 278, 1781–1784.

Parai, R., Mukhopadhyay, S., 2012. How large is the subducted water flux? New constraints on mantle regassing rates. Earth Planet. Sci. Lett. 317, 396–406.

Poirier, J.-P., 1994. Light elements in the Earth's core: A critical review. Phys. Earth Planet. Inter. 85, 319–337.

Rozel, A.B., Golabek, G.B., Jain, C., Tackley, P.J., Gerya, T., 2017. Continental crust formation on early Earth controlled by intrusive magmatism. Nature 545, 332–335, http://dx.doi.org/10.1038/nature22042.

Rüpke, L.H., Phipps Morgan, J., Hort, M., Connolly, J.A.D., 2004. Serpentine and the subduction zone water cycle. Earth Planet. Sci. Lett. 223, 17–34.

Sandu, C., Lenardic, A., McGovern, P., 2011. The effects of deep water cycling on planetary thermal evolution. J. Geophys. Res. 116, B12404, http://dx.doi.org/10.1029/2011JB008405.

Townend, J.P., Tsuchiya, J., Bina, C.R., Jacobsen, S.D., 2016. Water partitioning between bridgmanite and postperovskite in the lowermost mantle. Earth Planet. Sci. Lett. 454, 20–27, http://dx.doi.org/10.1016/j.epsl.2016.08.009.

Trackley, P.J., 2008. Modelling compressible mantle convection with large viscosity contrasts in a three-dimensional spherical shell using the yin-yang grid. Phys. Earth Planet. Inter 171, 7–18, http://dx.doi.org/10.1016/j.pepi.2008.08.005.

Xie, S., Tackley, P.J., 2004. Evolution of U–Pb and Sm–Nd systems in numerical models of mantle convection. J. Geophys. Res. 109, B11204, http://dx.doi.org/10.1029/2004JB003176.

Yamazaki, D., Karato, S., 2001. Some mineral physics constraints on the rheology and geothermal structure of Earth's lower mantle. Am. Mineral. 86, 301–385.

Zhong, S., Watts, A.B., 2013. Lithospheric deformation induced by loading of the Hawaiian Islands and its implications for mantle rheology. J. Geophys. Res. 118, 6025–6048, http://dx.doi.org/10.1002/2013JB010408.